Artvin Çoruh Üniversitesi
Doğal Afetler Uygulama ve Araştırma Merkezi
Doğal Afetler ve Çevre Dergisi

Artvin Çoruh University
Natural Hazards Application and Research Center
Journal of Natural Hazards and Environment

Araştırma Makalesi / Research Article, Doğ Afet Çev Derg, 2025; 11(1): 34–43, DOI: 10.21324/dacd.1455994

Spatial and Temporal Analysis of Earthquake Events in Kahramanmaraş on 6 February 2023

Özer Akyürek[1,*]

[1]*Kocaeli University, Faculty of Engineering, Department of Geomatics, 41001, Kocaeli, Türkiye.*

Abstract

Earthquakes are one of the most destructive natural disasters that occur as a result of the energy resulting from the movements of the earth's crust spreading and shaking the earth's surface. Since it is not possible to predict when and where earthquakes will occur, it has become possible to make various inferences and take necessary precautions by analyzing previous earthquakes. Spatial and temporal analysis of natural disasters such as earthquakes with geographic information systems provides useful information to local and global decision-makers in measures to be taken and mitigation studies. The objective of this study is to demonstrate that the general orientation of stress accumulation on fault lines can be monitored by weighted average centre points with the use of Geographic Information Systems (GIS). Spatio-temporal analyses of two earthquakes with a magnitude of 7.7 M_w and 7.6 M_w in Kahramanmaraş and aftershocks were performed. Ten-week spatial distributions of the aftershocks were examined with the weighted average center method and it was determined that the earthquake intensity and average centers shifted towards the north. When the spatial distribution of the earthquake centers is examined with the help of standard deviation ellipses weekly, it has been determined that they show orientation along the Eastern Anatolian Fault System.

Keywords

Earthquake, GIS, Spatiotemporal Analysis, Standard Deviational Ellipse, Weighted Average Center

6 Şubat 2023 Kahramanmaraş Depremlerinin Konumsal ve Zamansal Analizi

Özet

Depremler, yerkabuğunun hareketleri sonucu ortaya çıkan enerjinin yeryüzüne yayılması ve yeryüzünü sarsması sonucu meydana gelen en yıkıcı doğal afetlerden biridir. Depremlerin ne zaman ve nerede meydana geleceğini önceden kestirmek mümkün olmadığından, daha önce meydana gelmiş depremleri analiz ederek çeşitli çıkarımlar yapmak ve gerekli önlemleri almak mümkün olabilmektedir. Deprem gibi doğal afetlerin coğrafi bilgi sistemleri ile konumsal ve zamansal analizi, alınacak önlemlerde ve zarar azaltma çalışmalarında yerel ve küresel karar vericilere faydalı bilgiler sağlamaktadır. Bu çalışmada, Coğrafi Bilgi Sistemleri yardımıyla fay hatları üzerindeki stres birikiminin genel yöneliminin ağırlıklı ortalama merkez noktaları ile izlenebileceği gösterilmeye çalışılmıştır. Kahramanmaraş'ta meydana gelen 7.7 ve 7.6 M_w büyüklüğündeki iki depremin ve artçı şokların konumsal-zamansal analizleri yapılmıştır. Artçı depremlerin on haftalık konumsal dağılımları ağırlıklı ortalama merkez yöntemi ile incelenmiş ve geçen süreyle birlikte deprem yoğunluğu ile ortalama merkezlerinin kuzeye doğru kaydığı belirlenmiştir. Deprem merkezlerinin konumsal dağılımları haftalık standart sapma elipsleri yardımıyla incelendiğinde Doğu Anadolu Fay Sistemi boyunca yönelim gösterdikleri tespit edilmiştir.

Anahtar Sözcükler

Deprem, CBS, Konumsal-Zamansal Analiz, Standart Sapma Elipsi, Ağırlıklı Ortalama Merkez

1. Introduction

Two earthquakes, with magnitudes of 7.7 and 7.6 M_w, occurred on the Amanos and Pazarcık segments and the Sürgü - Çardak fault of the Eastern Anatolian Fault System (EAFS), respectively, at 01:17:32 (UTC) and 10:24:47 (UTC) on 6 February 2023, with epicenters in the Pazarcık and Elbistan districts of Kahramanmaraş. The magnitude of the first earthquake was measured as Mw = 7.8 by the USGS. The earthquake, which affected an area of 108,812 km^2 covering 11 provinces in the Eastern and Southeastern Anatolia Regions, caused severe damage or destruction to 33,143 buildings and over 50,000 deaths, more than 100,000 people were injured (AFAD 2023a, 2023b; Alkan et al., 2024). According to a report published by the Strategy and Budget Directorate of the Presidency of the Republic of Türkiye, the total cost of earthquakes to the Turkish economy is estimated at 103.6 billion USD (Strategy and Budget Directorate, 2023).

Earthquakes are one of the most destructive and deadly natural disasters on earth. Earthquake is defined as the sudden release of energy due to fractures in the earth's crust, spreading in waves and shaking the earth. Although it is impossible to predict where and when earthquakes will occur, recent research has shown that trends in earthquake risk in a particular

* Sorumlu Yazar: Tel: +90 (262) 3033247 Faks: +90 (262) 3033003
E-posta: ozer.akyurek@kocaeli.edu.tr (Akyürek Ö)

Gönderim Tarihi / Received : 20/03/2024
Kabul Tarihi / Accepted : 04/09/2024

region can be analyzed by examining the spatiotemporal processes of earthquake events. The results of the studies provide useful information for disaster prevention and mitigation. To reduce the destructive effects of earthquakes, precautions to be taken beforehand are of critical importance. For this reason, spatial and temporal analysis methods of Geographic Information Systems (GIS), which have been frequently preferred in recent years, are important methods that provide information for the measures to be taken. The results obtained as a result of spatial and temporal analysis using GIS provide valuable information to decision-makers at global and local scales. Earthquake events can be considered as data with geographical attributes. Traditional statistical analysis techniques are unable to characterize the constraint relationships between spatial data because of the spatial limitations imposed by varying directions and distances between these data. By merging the statistics of spatial data with contemporary graphical computing technology and applying heuristic approaches, spatial statistics may display the spatial distribution, spatial pattern, and spatial relationships in spatial data (Shan et al., 2021).

In the literature, there are studies conducted in many different areas by using spatial and temporal analysis methods of GIS. Wang et al., (2012) examined China's food production spatially and temporally using the weighted average center method. They determined the directions in which the production of various food groups has shifted over time within the study region. Al-Kindi et al., (2017) analyzed Dubas insect infestation data in northern Oman over ten years with spatial and temporal methods of GIS. During the study period, they determined the movement directions of insect infestation by performing analysis according to the years with the weighted average center method. Xu et al., (2018) investigated impervious surface variations in Guangzhou, China, with the help of weighted average center and standard deviation ellipses. In the period between 1988 and 2015, the principle orientation, direction, spatiotemporal expansion trends, and distribution differences of impermeable surfaces were revealed on the maps they created. Çolak & Sunar, (2020) spatially and temporally analyzed the forest fires occurring in the Muğla-Marmaris and İzmir-Menderes regions of Türkiye using data from the NASA FIRMS database. They concluded that the fire risk of the Marmaris region is higher than the Menderes region. Cheng et al., (2022) performed a spatial and temporal analysis of economic resilience in Chinese cities during the COVID-19 pandemic. As a result of their analysis, they found that the spatial distribution of economic resilience showed a tendency towards clustering and trended from SE to NW, and the weighted average centers shifted from NW to SE. Zhang et al., (2022) investigated the destructive effects of the earthquake that occurred in Longtoushan, China in 2014 on buildings and people with spatial analysis. The studies carried out after various natural disasters can be shown as proof of how effective the GIS methods produce information. Ocaña et al., (2008) performed spatial and temporal analyses of the earthquake and its aftershocks that occurred in the town of La Paca in southeastern Spain. After their analysis, they determined that the distribution of aftershocks developed trends in three different directions. Veitch & Nettles, (2012) conducted spatial and temporal analysis of earthquakes occurring in the Greenland polar region. They analyzed the spatial and temporal trends of earthquakes occurring in 18 years. Santos et al., (2014) analyzed flood and landslide events in the north of Portugal with the help of spatial analysis of GIS. They determined that natural disaster events increased by 0.17 per decade with the help of trend analysis. Yang et al., (2017) examined the spatial and temporal analysis of landslide events occurring around the earthquake center after large earthquakes using geographic information systems and remote sensing techniques. Dias et al., (2019) examined the effect of considering partial sets of data on the spatiotemporal probability distributions of earthquakes using earthquake data on the California San Andreas fault. Huang et al., (2020) spatially and temporally analyzed the precursor earthquakes that occurred before the magnitude 6.4 and 7.1 M earthquakes that occurred in Ridgecrest, California in 2019. They obtained information about the orientations of the foreshocks. Shan et al., (2021) analyzed the temporal and spatial analysis of earthquakes occurring on the San Andreas fault for forty years. They analyzed the earthquakes, which they divided into certain periods, according to the weighted average center method. They also examined the clustering of earthquakes with the help of spatial autocorrelation analysis. Ferreira et al., (2022) investigated the correlation between earthquakes by performing a spatiotemporal analysis of real and synthetic earthquake data. Sarfraz et al., (2023) analyzed the spatiotemporal distribution of landslides in a region in northern Pakistan using various satellite images and GIS.

If local governments have a solid understanding of the temporal and spatial development rules of seismic events in a particular region with frequent earthquakes, they can make informed decisions on disaster prevention and mitigation for that region. Thus, they can take necessary precautions and make decisions to ensure the life safety of the people living in and around the region. This is why, the accurate information is the most important data source in such cases. For this reason, this study aims to determine the weekly orientation of aftershocks occurring after two major earthquakes in Kahramanmaraş in order to produce information for disaster prevention and mitigation. Therefore, the weekly trend of earthquake intensity was followed by spatially and temporally analyzing the aftershocks occurring for ten weeks after two large earthquakes occurring a few hours apart using the weighted average center method. With this method, it has been determined in which directions the aftershocks may cause stress accumulation on the fault lines where they occur. In addition, the weekly standard deviation ellipses of the earthquakes were analyzed and the trend orientations of the aftershocks were analyzed.

2. Materials and Methods

2.1. Study area

The study area is Kahramanmaraş and its neighboring provinces in Türkiye, located on the EAFS, where earthquakes with magnitudes of 7.7 and 7.6 Mw occurred a few hours apart on 06.02.2023 (Figure 1). EAFS forms an NE-SW left-lateral strike-slip boundary between the northward-moving Arabian Plate and the westward-moving Anatolian Block. The EAFS and the North Anatolian Fault System (NAFS), which are among the most active and active fault systems in Türkiye, form the boundary between the Anatolian and Arabian Plates, causing the Anatolian block to move westward. Current GPS data gives a present-day slip rate in the range of 11±2 mm/year (Aksoy et al., 2007; Arpat & Şaroğlu, 1972; Jackson & McKenzie, 1984; Lyberis et al., 1992; Nalbant et al., 2002; Şaroğlu et al., 1992; Şengör et al., 1985; Westaway, 2003). The EAFS extends as a single segment from Karlıova (Kargapazarı) in the northeast to the west of Çelikhan. The southern segment of the fault, which is split into two parts, continues from north of the Gölbaşı Basin and Pazarcık to southwest of the Türkoğlu. The fault leaps to the right south of Türkoğlu and continues by bounding Sağlık, Kocagöl, and Amik plains from the west and ends by scattering south of Kırıkhan. In this region of the EAFS, the depression basin that includes the Sağlık and Narlı plains is bounded from the east by the Sakçagöz and Narlı segments of the Dead Sea Fault Zone. The Narlı section extends N-NE for 30-40 km from north of the Pazarcık to the EAFS. The northern segment, which diverges west of Çelikhan, forms a northward convex line by the morphology of the southeastern Toros Mountain Belt. This segment consists of Sürgü and Çardak faults and Savrun, Çokak and Toprakkale faults turning to SW from Göksun (AFAD, 2023a).

After the two main earthquakes, 27925 aftershocks of various magnitudes occurred in the region during the ten-week study period. Statistical information about the earthquakes is shown in Table 1, while earthquake locations and fault lines are shown in Figure 1.

Table 1: Statistics on the frequency of earthquake events over different weeks (AFAD, 2023c)

Weeks (2023)	Number of Earthquakes	Magnitude 0.2 – 2.0 (M_w)	Magnitude 2.0 – 3.0 (M_w)	Magnitude 3.0 – 4.0 (M_w)	Magnitude 4.0 – 5.0 (M_w)	Magnitude 5.0 – 7.7 (M_w)
First (06-12/02)	3907	20	1760	1705	370	52
Second (13-19/02)	3647	163	2795	649	36	4
Third (20-26/02)	3742	318	2939	450	33	2
Fourth (27/02-05/03)	3213	426	2527	238	21	1
Fifth (06-12/03)	2734	371	2139	212	12	–
Sixth (13-19/03)	2529	466	1897	155	11	–
Seventh (20-26/03)	2309	419	1737	141	11	1
Eighth (27/03-02/04)	2200	357	1700	134	9	–
Ninth (03-09/04)	1860	368	1389	99	4	–
Tenth (10-16/04)	1784	348	1342	89	5	–

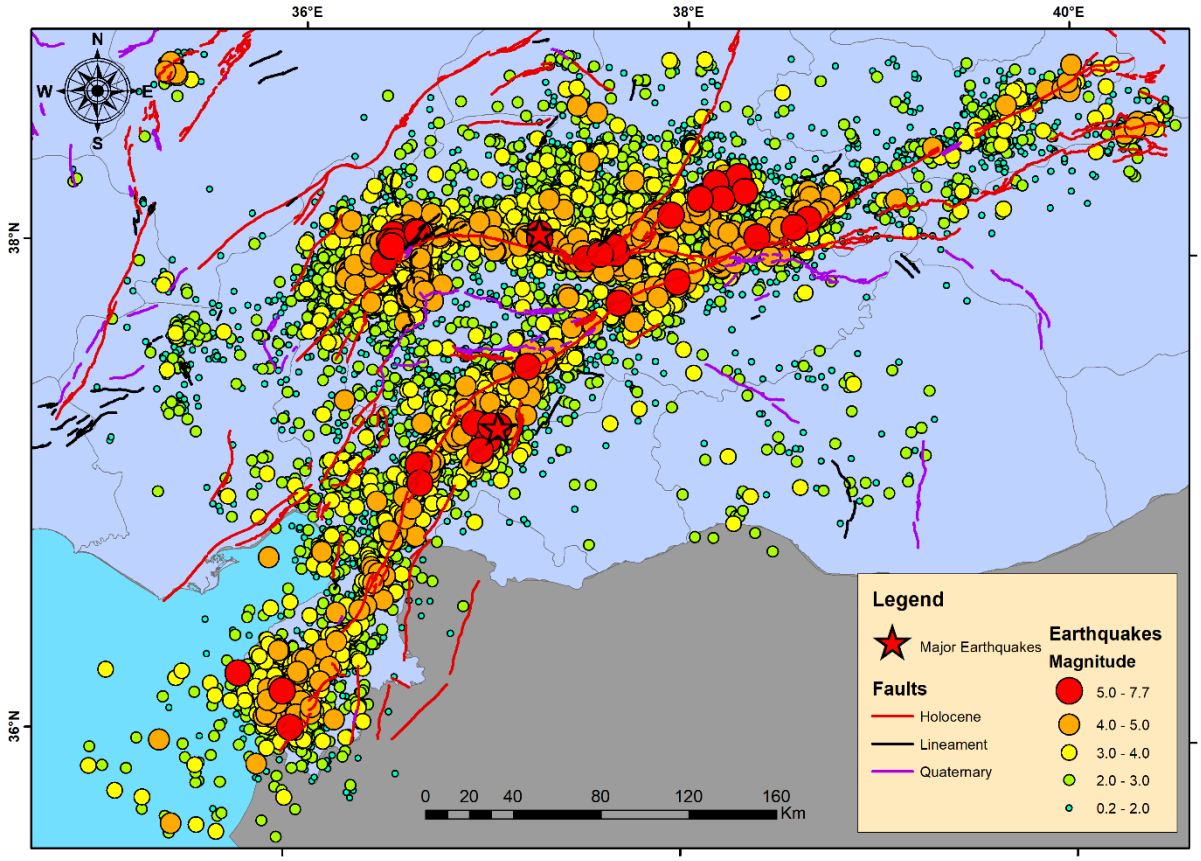

Figure 1: 6 February Kahramanmaraş Pazarcık and Elbistan major earthquakes and aftershocks and Eastern Anatolian Fault System where the earthquakes occurred

2.2. Methods

In the study, firstly, the transformation process was carried out to ensure the integrity of the earthquake data. All magnitude units in the earthquake catalog data received from the Ministry of Interior Disaster and Emergency Management Presidency (AFAD), the data provider institution, were converted to Mw. Afterward, weekly average center points were calculated with earthquake magnitudes as weight values. Finally, standard deviation ellipses were created with the weekly earthquakes, and the weekly orientations of the aftershocks were monitored.

2.2.1. M_L – M_w conversion

Firstly, earthquake magnitude unit conversion was performed to ensure the integrity of the study within the dataset. All earthquake magnitudes in the M_L unit in the data set were converted to the M_w unit with the formulas taken from the studies given below. For small earthquakes $0 \leq M_L \leq 3.8$ (Munafò et al., 2016) mentioned the following formula;

$$M_w=(2/3)*M_L+1.15 \quad (1)$$

and (Kadirioğlu & Kartal, 2016) mentioned their study for the earthquake ranges $3.3 \leq M_L \leq 6.6$ following the formula;

$$M_w=0.8095*M_L+1.3003 \quad (2)$$

was used for the conversion from M_L to M_w.

2.2.2. Weighted average center

The mean center, used in spatial analysis, is the average geographic coordinates of all features in the dataset. It is a useful tool for tracking changes in the distribution of features within the dataset. The mean center method is also significantly affected by outliers in the dataset and when a feature is found more than once in the same location. On the other hand, the weighted mean center method used in spatial analysis is defined as the geographic center of a set of points arranged according to the influence of a value associated with each dataset feature. The weighted mean center method is used to reflect the importance of each feature in a data set and its influence on the overall distributional trend of the data set.

The method requires that a feature in the data set is assigned a weight value. The assigned weight value indicates the importance of the feature in the data set. The weighted mean value of the data set is then calculated by multiplying each feature by its weight value, summing it up, and dividing this sum by the sum of all weights. The weighted mean center extends to the following;

$$\bar{X}=\frac{\sum_{i=1}^{n} w_i x_i}{\sum_{i=1}^{n} w_i}$$
$$\bar{Y}=\frac{\sum_{i=1}^{n} w_i y_i}{\sum_{i=1}^{n} w_i} \quad (3)$$

where x_i and y_i are the latitude and longitude coordinates of the earthquake event *i*, respectively; *n* is the total number of earthquake events in different weeks; and w_i is the magnitude of earthquake event *i* (Delmelle, 2009; Mitchell, 2005).

2.2.3. Standard deviational ellipse

Standard deviation ellipses are used to describe the spatial distribution and orientation of geographic features in a given study area. The Standard Deviation Ellipse is used to determine the direction of distribution of data in the study area (Shan et al., 2021). In a standard deviation ellipse, which is commonly used to measure the trend of features of a dataset, the distance is calculated separately in the x and y geographic coordinate direction. The distance value calculated in these two directions defines the axes of an ellipse covering the feature distribution. The method works by calculating the standard deviation of the x and y coordinates from the mean center to define the axes of the ellipse. The ellipse allows us to observe the length of the distribution of the dataset and therefore whether there is a specific orientation. The axis directions of the ellipse provide information about the direction of the spatial distribution of geographic elements (earthquake centers). The difference between the major axis and the minor axis carries information about the directionality of geographic elements. If the length of the major axis is equal to the length of the minor axis, there is no directional change in the distribution of geographic elements. The standard deviational ellipse is given as:

$$\sigma_{1,2}=\left(\frac{\left(\sum_{i=1}^{n}\tilde{x}_i^2+\sum_{i=1}^{n}\tilde{y}_i^2\right)\pm\sqrt{\left(\sum_{i=1}^{n}\tilde{x}_i^2-\sum_{i=1}^{n}\tilde{y}_i^2\right)^2+4\left(\sum_{i=1}^{n}\tilde{x}_i\tilde{y}_i\right)^2}}{2n}\right)^{1/2} \quad (4)$$

where *x* and *y* are the coordinates for earthquake event *i*, $\{\bar{x}, \bar{y}\}$ represent the mean center for the earthquake events and *n* is equal to the total number of earthquake events (Delmelle, 2009; Mitchell, 2005; Wang et al., 2015).

3. Results

In this study, it was aimed to monitor the weekly distributions and trends of aftershocks that occurred after two consecutive major earthquakes (M_w > 7.0). To achieve this aim, the weekly movements of the aftershocks that occurred during the study period were monitored with the weighted average center method. Figure 2 shows the weekly weighted average center points. Accordingly, the weighted average center points were geographically located in the middle region of the two main earthquakes. When the weekly locations of the weighted average center points are examined, it is seen that a northward movement has occurred. Table 2 shows the weekly movement directions and distances of the weighted average center points. During the ten-week study period, the weighted average center of the earthquakes shifted 16.80 km to the north at an angle of 7°. When Figure 2 is analyzed, it is seen that only the third-week moves towards the south-east. This is due to the 6.4 M_w earthquake that occurred in Hatay province (southeast of the study area) in the third week of the study and the high number of aftershocks that occurred afterward.

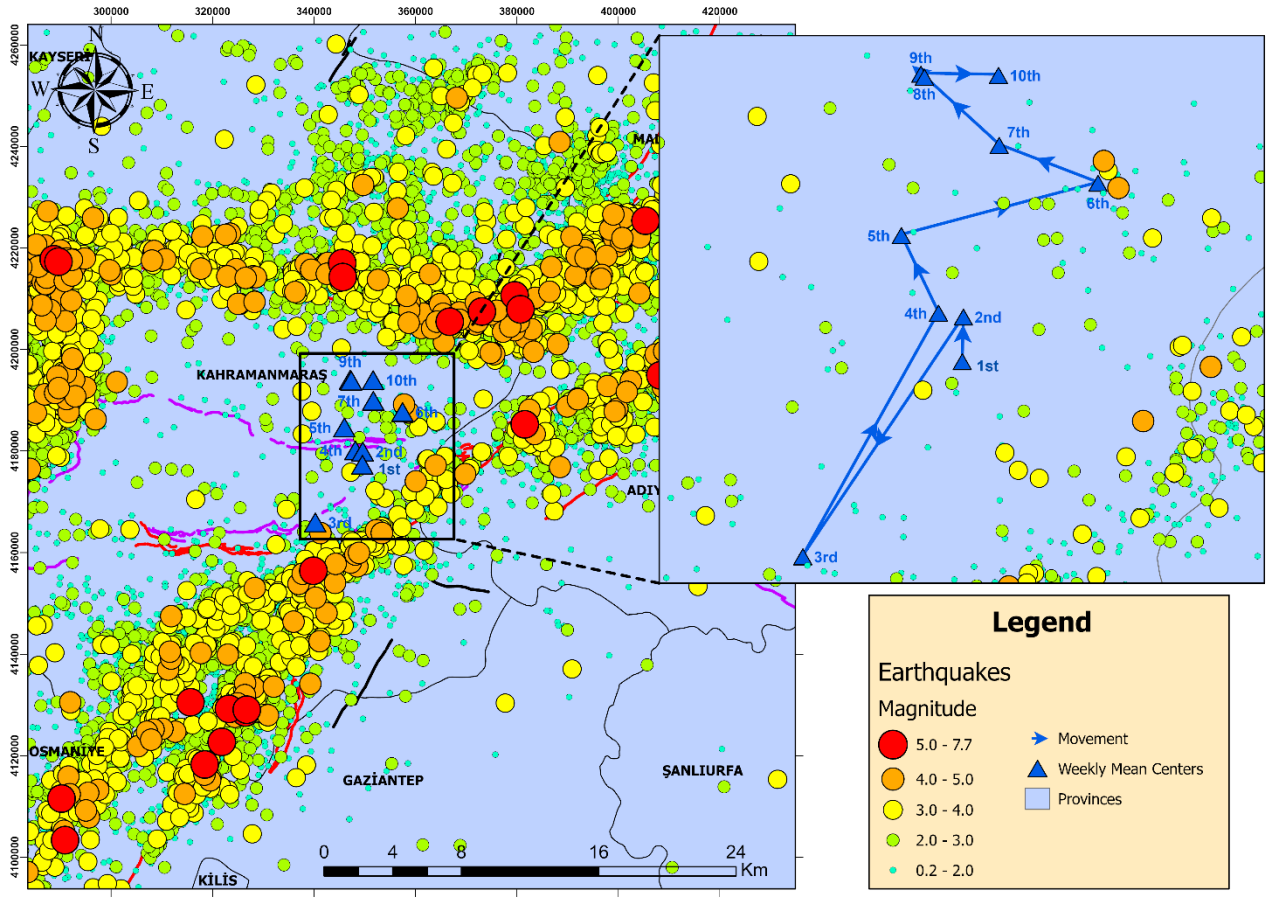

Figure 2: The weighted average center's temporal and spatial evolution process for earthquake events

Table 2 shows that the weighted average center points moved a total of 69.34 km and each segment moved in a northerly direction, except for the third week.

Table 2: Movement directions and distances of the weighted average centers according to different weeks

Weeks	Segment (km)	Directions
First	–	
Second	2.60	N
Third	16.80	SW
Fourth	16.23	NE
Fifth	5.01	NW
Sixth	11.85	NE
Seventh	6.17	NW
Eighth	5.89	NW
Ninth	0.27	NW
Tenth	4.52	E
Total	69.34	N – NE

One of the most remarkable and important risk mitigation information that the study provides to decision-makers is that the orientation of the stress generated by an earthquake on a fault can be tracked by weighted average center points. According to Toda et al. (2023), the most likely scenario is that aftershocks will remain clustered in the stress-triggering lobes, and while their number will decrease according to Omori's law, their magnitude will not necessarily decrease. When Figure 2 is examined, the fact that the weighted average center point of the second week shifted to the north supports this situation. The reason for the shift of the weighted average center point of the third week by 16.8 km to the south-east can be attributed to the 6.4 M_w Hatay earthquake, which is likely to have occurred due to stress accumulation at the southern end of the EAFS, and the aftershocks that followed.

The continuous northward movement of the weighted average center points in the following weeks can be interpreted as a sign of increased stress accumulation in the northern branch of the EAFS and stress accumulation in this region, which has produced large earthquakes in previous years. February 6 earthquakes may have transferred energy to two fault systems in particular. These fault lines are the Eastern Anatolian Fault System, which radiates down towards the Adana basin, and the Malatya Fault System, which extends west of Malatya in the direction of Doğanşehir-Kepez-Başkavak-Kemaliye. The Malatya Fault system mentioned here is located north of the study area of this study. The situation mentioned here is in parallel with the results obtained in this study.

In standard deviation ellipses, the deviation along the major axis represents the direction of maximum spread of points and the deviation along the minor axis represents the direction of minimum spread of points. Figure 3 shows the weekly standard deviation ellipses of aftershocks. The statistical parameter analysis results of the SDE in weeks are listed in Table 3. The azimuth angle of the SDE provides information about the main trend direction of the distribution of earthquake points. The weekly SDE rotation angles shown in Table 3 are distributed between 50° and 65°. This indicates that the dominant distribution direction of the earthquake centers is NE-SW, i.e. parallel to the EAFS direction. When Figure 3 and Table 3 are analyzed, it is seen that the SDEs of the weeks other than the third and fifth weeks have similar values. The reason why the main axis of the ellipse belonging to the third week is longer than the others can be shown as the high number of aftershocks after the earthquake in Hatay. It is observed that earthquakes occurring in this region increase the area and major axis value of the SDE. What is noteworthy is the SDE of the fifth week, which has the highest area and small axis value. The reason for this situation is the high number and magnitudes of earthquakes that occurred as a result of the stresses accumulated on the Savrun fault located southwest of the Çardak fault, the fault where the second main earthquake occurred.

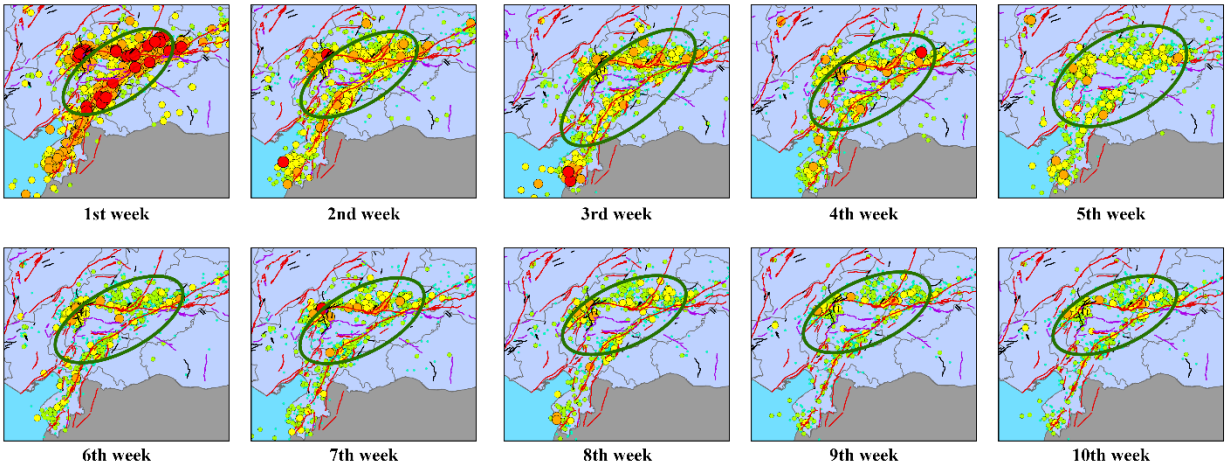

Figure 3: The SDEs of seismic occurrences evolve both spatially and temporally

Table 3: Results of the SDE's statistical parameter analysis of the earthquake events during the different weeks

Weeks	Area (km^2)	XSD (km)	YSD (km)	Rotation (°)
First	20590.81	117.694	55.692	56.11
Second	21798.43	122.372	56.703	58.55
Third	30894.11	152.509	64.484	50.77
Fourth	26159.70	131.545	63.303	57.68
Fifth	32799.08	135.758	76.906	61.11
Sixth	24421.96	131.079	59.308	62.07
Seventh	23792.67	127.520	59.393	61.68
Eighth	22618.05	123.693	58.207	65.67
Ninth	22632.37	123.755	58.215	65.82
Tenth	24266.82	129.472	59.663	63.61

The difference between this study from similar studies in the literature is that the spatial and temporal analysis of the aftershocks that occur after large earthquakes with high destructive effects can determine the orientations on the fault lines and suggest the necessary special measures to be taken in the residential areas that coincide with these regions. In addition, it is an important source of information for monitoring the direction of stress accumulated on fault lines outward from the earthquake point as a result of large earthquakes and taking the necessary precautionary steps accordingly.

4. Discussion

This study offers a different approach to investigating the temporal and spatial evolution trends of earthquakes and understanding the earthquake risk in a given region. The experimental results of the temporal and spatial evolution trends in this paper are consistent with the following researches, which demonstrate the validity of using the spatial statistical method to study the spatial and temporal evolution characteristics of earthquake events.

Toda et al. (2023) reported that the first earthquake of magnitude 7.7 was not the main cause of the second earthquake of magnitude 7.6, but it supported the occurrence of the second earthquake. In parallel with this, according to the findings obtained as a result of the analyses performed in this study, the fact that the weighted average center points have shifted to the north supports that stress accumulation may have increased at the northern end of the EAFS. Kobayashi et al. (2023), Över et al. (2023), Tikhotsky et al. (2023), He et al. (2023), Utkucu et al. (2023), Rebetsky (2023), Alkan et al. (2024), Dai et al. (2024) and Li et al. (2024) in their coulomb stress analyses, showed that the stress accumulations after the main earthquakes were north oriented.

The standard deviation ellipses revealed that the main trend directions of the aftershocks were parallel to the EAFS. Similarly, Shan et al. (2021) and Huang et al. (2020) found parallels along the fault line in the SDEs they generated with historical earthquakes on the San Andreas fault.

Earthquake catalogues are important for determining the temporal and spatial evolution characteristics of earthquake events; the more complete the earthquake catalogue, the more accurate the research results will be. Therefore, maintaining earthquake catalogues regularly, precisely and above a certain accuracy will play an important role in the accuracy of the results of this and similar studies.

5. Conclusions

In this study, the spatial and temporal analyses of the earthquakes with magnitudes of 7.7 and 7.6 M_w that occurred in Kahramanmaraş on 06.02.2023 were performed. In the analyses performed using weighted mean center and standard deviation ellipses, the orientation of the aftershocks was examined and the direction of the stress accumulation that may be caused by fault lines was investigated. When the weighted average center approach was used to analyze the ten-week spatial distributions of the aftershocks, it was found that both the average centers and the earthquake strength changed northward. It has been found that the standard deviation ellipses weekly are useful in examining the spatial distribution of earthquake centers, which exhibit direction along the Eastern Anatolian Fault System.

The unique aspect of this paper is the demonstration that the general orientation of stress accumulation on fault lines can be tracked by weighted average center points. This and similar information is very important to protect and save the lives of people living in settlements built on or near fault lines. The priority of such information is of great importance in producing policies and making decisions to reduce the damages of natural disasters and to overcome them with minimum loss of life and property. Since the location and time of earthquakes cannot be known or predicted with certainty, the value of the information produced as a result of spatial and temporal analysis supported by such geographic information systems becomes even more important. The information produced in this way will play an effective role in the measures to be taken by local and general decision-makers.

Acknowledgments

The author is thankful to the Republic of Turkey–Ministry of Interior Disaster and Emergency Management Authority (AFAD) for providing the data.

References

AFAD. (2023a). *06 February 2023 Kahramanmaraş (Pazarcık and Elbistan) earthquakes field studies preliminary evaluation report*. Republic of Turkey Ministry of Interior Disaster and Emergency Management Presidency. Retrieved March 7, 2024, from https://deprem.afad.gov.tr/assets/pdf/Arazi_Onrapor_28022023_surum1_revize.pdf

AFAD. (2023b). *Preliminary evaluation report on 06 February 2023 Pazarcık (Kahramanmaraş) Mw 7.7 and Elbistan (Kahramanmaraş) Mw 7.6 earthquakes*. Republic of Turkey Ministry of Interior Disaster and Emergency Management Presidency. Retrieved March 7, 2024, from https://deprem.afad.gov.tr/assets/pdf/Kahramanmara%C5%9F%20Depremi%20%20Raporu_02.06.2023.pdf

AFAD. (2023c). *AFAD deperem katalogu*. Retrieved March 7, 2024, from https://deprem.afad.gov.tr/event-catalog

Aksoy, E., Inceöz, M., & Koçyiğit, A. (2007). Lake Hazar basin: A negative flower structure on the East Anatolian Fault System (EAFS), SE Turkey. *Turkish Journal of Earth Sciences*, *16*(3), 319–338.

Al-Kindi, K. M., Kwan, P., Andrew, N. R., & Welch, M. (2017). Modelling spatiotemporal patterns of dubas bug infestations on date palms in northern Oman: A geographical information system case study. *Crop Protection*, *93*, 113–121. https://doi.org/10.1016/j.cropro.2016.11.033

Alkan, H., Büyüksaraç, A., & Bektaş, Ö. (2024). Investigation of earthquake sequence and stress transfer in the Eastern Anatolia Fault Zone by Coulomb stress analysis. *Turkish Journal of Earth Science. 33*(1), 56–68. https://doi.org/10.55730/1300-0985.1898

Arpat, E., & Şaroğlu, F. (1972). Some observations and thoughts on the East Anatolian Fault. *Bulletin of the Mineral Research and Exploration*, *78*(78), 44–50.

Cheng, T., Zhao, Y., & Zhao, C. (2022). Exploring the spatio-temporal evolution of economic resilience in Chinese cities during the COVID-19 crisis. *Sustainable Cities and Society*, *84*(126), Article 103997. https://doi.org/10.1016/j.scs.2022.103997

Çolak, E., & Sunar, F. (2020). The importance of ground-truth and crowdsourcing data for the statistical and spatial analyses of the NASA FIRMS active fires in the Mediterranean Turkish forests. *Remote Sensing Applications: Society and Environment*, *19*, Article 100327. https://doi.org/10.1016/j.rsase.2020.100327

Delmelle, E. (2009). Point pattern analysis. *International Encyclopedia of Human Geography*, 204–211. https://doi.org/10.1016/B978-008044910-4.00494-6

Dai, X., Liu, X., Liu, R., Song, M., Zhu, G., Chang, X., & Guo, J. (2024). Coseismic Slip Distribution and Coulomb Stress Change of the 2023 M_w 7.8 Pazarcik and M_w 7.5 Elbistan Earthquakes in Turkey. *Remote Sensing. 16*(2), Article 240. https://doi.org/10.3390/rs16020240

Dias, V. H. A., Papa, A. R. R., & Ferreira, D. S. R. (2019). Analysis of temporal and spatial distributions between earthquakes in the region of California through Non-Extensive Statistical Mechanics and its limits of validity. *Physica A: Statistical Mechanics and Its Applications*, *529*, Article 121471. https://doi.org/10.1016/j.physa.2019.121471

Ferreira, D. S. R., Ribeiro, J., Oliveira, P. S. L., Pimenta, A. R., Freitas, R. P., Dutra, R. S., Papa, A. R. R., & Mendes, J. F. F. (2022). Spatiotemporal analysis of earthquake occurrence in synthetic and worldwide data. *Chaos, Solitons and Fractals*, *165*(P2), Article 112814. https://doi.org/10.1016/j.chaos.2022.112814

He, L., Feng, G., Xu, W., Wang, Y., Xiong, Z., Gao, H., & Liu, X. (2023). Coseismic Kinematics of the 2023 Kahramanmaras, Turkey Earthquake Sequence From InSAR and Optical Data. *Geophysical Research Letters*, *50*(17), Article e2023GL104693. https://doi.org/10.1029/2023GL104693

Huang, H., Meng, L., Bürgmann, R., Wang, W., & Wang, K. (2020). Spatio-temporal foreshock evolution of the 2019 M 6.4 and M 7.1 Ridgecrest, California earthquakes. *Earth and Planetary Science Letters*, *551*, Article 116582. https://doi.org/10.1016/j.epsl.2020.116582

Jackson, J., & McKenzie, D. (1984). Active tectonics of the Alpine–Himalayan Belt between western Turkey and Pakistan. *Geophysical Journal of the Royal Astronomical Society*, *77*(1), 185–264. https://doi.org/10.1111/j.1365-246X.1984.tb01931.x

Kadirioğlu, F. T., & Kartal, R. F. (2016). The new empirical magnitude conversion relations using an improved earthquake catalogue for Turkey and its near vicinity (1900–2012). *Turkish Journal of Earth Sciences*, *25*(4), 300–310. https://doi.org/10.3906/yer-1511-7

Kobayashi, T., Munekane, H., Kuwahara, M., & Furui, H. (2023). Insights on the 2023 Kahramanmaraş Earthquake, Turkey, from InSAR: fault locations, rupture styles and induced deformation. *Geophysical Journal International*, *236*(2), 1068–1088. https://doi.org/10.1093/gji/ggad464

Li, W., Zhao, L., Tan, K., Lu, X., Zhang, C., Li, C., & Han, S. (2024). Coseismic deformation and fault slip distribution of the 2023 M_w 7.8 and M_w 7.6 earthquakes in Türkiye. *Earthquake Science*, *37*, 263–276. https://doi.org/10.1016/j.eqs.2024.03.006

Lyberis, N., Yurur, T., Chorowicz, J., Kasapoglu, E., & Gundogdu, N. (1992). The East Anatolian Fault: an oblique collisional belt. *Tectonophysics*, *204*(1), 1–15. https://doi.org/https://doi.org/10.1016/0040-1951(92)90265-8

Mitchell, A. (2005). *The ESRI Guide to GIS Analysis* (Volume 2). ESRI Press.

Munafò, I., Malagnini, L., & Chiaraluce, L. (2016). On the relationship between mw and mL for small earthquakes. *Bulletin of the Seismological Society of America*, *106*(5), 2402–2408. https://doi.org/10.1785/0120160130

Nalbant, S. S., McCloskey, J., Steacy, S., & Barka, A. A. (2002). Stress accumulation and increased seismic risk in Eastern Turkey. *Earth and Planetary Science Letters*, *195*(3–4), 291–298. https://doi.org/10.1016/S0012-821X(01)00592-1

Ocaña, E., Stich, D., Carmona, E., Vidal, F., Bretón, M., Navarro, M., & García-Jerez, A. (2008). Spatial analysis of the La Paca, SE Spain, 2005 seismic series through the relative location of multiplets and principal component analysis. *Physics of the Earth and Planetary Interiors*, *166*(3–4), 117–127. https://doi.org/10.1016/j.pepi.2007.12.005

Över, S., Demirci, A., & Özden, S. (2023). Tectonic implications of the February 2023 Earthquakes (Mw7.7, 7.6 and 6.3) in south-eastern Türkiye. *Tectonophysics*, *866*, Article 230058. https://doi.org/10.1016/j.tecto.2023.230058

Rebetsky, Y.L. (2023). Tectonophysical Zoning of Seismic Faults in Eastern Anatolia and February 6, 2023 Kahramanmaraş Earthquakes. *Izvestiya, Physics of the Solid Earth, 59*, 851-877. https://doi.org/10.1134/S1069351323060174

Santos, M., Bateira, C., Soares, L., & Hermenegildo, C. (2014). Hydro-geomorphologic GIS database in Northern Portugal, between 1865 and 2010: Temporal and spatial analysis. *International Journal of Disaster Risk Reduction*, *10*(PA), 143–152. https://doi.org/10.1016/j.ijdrr.2014.08.003

Sarfraz, Y., Basharat, M., Riaz, M. T., Akram, M. S., Ahmed, K. S., & Shahzad, A. (2023). Spatio-temporal evolution of landslides along transportation corridors of Muzaffarabad, Northern Pakistan. *Environmental Earth Sciences*, *82*(5), 1–23. https://doi.org/10.1007/s12665-023-10822-5

Şaroğlu, F., Emre, Ö., & Kuşçu, I. (1992). The East Anatolian fault zone of Turkey. *Annales Tectonicae*, *6*, 99–125.

Şengör, A.M.C., Görür, N., & Şaroğlu, F. (1985). Strike-Slip Faulting and Related Basin Formation in Zones of Tectonic Escape: Turkey as a Case Study. In K. T. Biddle & N. Christie-Blick (Eds.), *Strike-Slip Deformation, Basin Formation, and Sedimentation* (Vol. 37). SEPM Society for Sedimentary Geology. https://doi.org/10.2110/pec.85.37.0211

Shan, W., Wang, Z., Teng, Y., & Wang, M. (2021). Temporal and spatial evolution analysis of earthquake events in california and nevada based on spatial statistics. *ISPRS International Journal of Geo-Information*, *10*(7), Article 465. https://doi.org/10.3390/ijgi10070465

Strategy and Budget Directorate. (2023). *2023 Kahramanmaraş ve Hatay Earthquake Reports*. Presidency of the Republic of Turkey Strategy and Budget Department. Retrieved March 7, 2024, from https://www.sbb.gov.tr/wp-content/uploads/2023/03/2023-Kahramanmaras-ve-Hatay-Depremleri-Raporu.pdf

Tikhotsky, S. A., Tatevosyan, R. E., Rebetsky, Y. L., Ovsyuchenko, A. N., & Larkov, A. S. (2023). The 2023 Kahramanmaraş Earthquakes in Turkey: Seismic Movements along Conjugated Faults. *Doklady Earth Sciences*, *511*, 703–709. https://doi.org/10.1134/S1028334X23600974

Toda, S., Stein, R. S., Özbakır, A. D., Gonzalez-Huizar, H., Sevilgen, V., Lotto, G., & Sevilgen, S. (2023). Stress change calculations provide clues to aftershocks in 2023 Türkiye earthquakes. *Temblor*. https://doi.org/http://doi.org/10.32858/temblor.295

Utkucu, M, Durmuş, H., Uzunca, F., & Nalbant, S. (2023). *A Preliminary Report on the 2023 Gaziantep (Mw=7.7) and Elbistan (Mw=7.5) Earthquakes in Souhteast Türkiye.* Sakarya University Disaster Management Application and Research Centerand Department of Geophysics. Retrieved March 7, 2024, from https://jfm.sakarya.edu.tr/sites/jfm.sakarya.edu.tr/file/Rapor1.pdf

Veitch, S.A., & Nettles, M. (2012). Spatial and temporal variations in Greenland glacial-earthquake activity, 1993-2010. *Journal of Geophysical Research: Earth Surface*, *117*(4), 1993–2010. https://doi.org/10.1029/2012JF002412

Wang, B., Wenzhong, S., & Zelang, M. (2015). Confidence Analysis of Standard Deviational Ellipse and Its Extension into Higher Dimensional Euclidean Space. *PLoS ONE2*, *10*(3), Article e0118537. https://doi.org/https://doi.org/10.1371/journal.pone.0118537

Wang, Q., Yue, T.X., Wang, C.L., Fan, Z.M., & Liu, X.H. (2012). Spatial-temporal variations of food provision in China. *Procedia Environmental Sciences*, *13*(2011), 1933–1945. https://doi.org/10.1016/j.proenv.2012.01.187

Westaway, R. (2003). Kinematics of the Middle East and Eastern Mediterranean updated. *Turkish Journal of Earth Sciences*, *12*(1), 5–46.

Xu, J., Zhao, Y., Zhong, K., Zhang, F., Liu, X., & Sun, C. (2018). Measuring spatio-temporal dynamics of impervious surface in Guangzhou, China, from 1988 to 2015, using time-series Landsat imagery. *Science of the Total Environment*, *627*, 264–281. https://doi.org/10.1016/j.scitotenv.2018.01.155

Yang, W., Qi, W., Wang, M., Zhang, J., & Zhang, Y. (2017). Spatial and temporal analyses of post-seismic landslide changes near the epicentre of the Wenchuan earthquake. *Geomorphology*, *276*, 8–15. https://doi.org/10.1016/j.geomorph.2016.10.010

Zhang, L., Tao, Z., & Wang, G. (2022). Assessment and determination of earthquake casualty gathering area based on building damage state and spatial characteristics analysis. *International Journal of Disaster Risk Reduction*, *67*, Article 102688. https://doi.org/10.1016/j.ijdrr.2021.102688